

Chapter 2

State of the Art

Contemporary engineering sciences are strictly related to the broad application of computer technologies and methods. The finite difference method (FDM), the boundary element method (BEM) and the finite element method (FEM) are the most popular computational methods. The FEM is certainly the most widely used, which is proven by the numerous computing systems based on this method that are applied in engineering practice. Attempts are being made to model not only changes occurring within the material being processed, but also within the forming tool, which enables a final product of very good quality to be obtained. Such attempts are possible, first and foremost, thanks to the use of mathematical modelling for the occurring physical phenomena. Mathematical models combined with the finite element method provide great possibilities for the modelling of metal deformation processes even for complicated shapes of the deformation zone and complex thermal conditions [1–3]. They may also be applied for effects that occur during the semi-solid steel deformation process. In actual metal working processes, a number of effects occur in parallel, such as the metal flow, metal temperature changes, heat generation as a result of plastic deformation work, friction force work, heat discharge as a result of contact between the metal deformed and the tool, or heat discharge to the environment by radiation and convection. For hot plastic working, the metal mechanical properties considerably depend on the temperature. A substantial irregularity of deformation in some processes leads to uneven heat generation, and consequently to an uneven structure and metal properties. In addition, the contact of the hot metal with a cold tool causes that high temperature gradients develop in the vicinity of the contact surface [2]. Phase transformations, both in the liquid and the solid state, are additional, temperature dependent factors which may influence the process. They may significantly influence both the deformation resistance and the grain size, as well as the metal properties after the plastic working. At present, there are many mathematical models and computer simulation programmes for processes occurring within the temperature range typical of the cold and hot working. An example of a solution, assuming a rigid-plastic model of the body deformed, may be found in publications concerning rolling

[4–6], upsetting [7, 8], or drawing [9]. Only in recent years have solutions to the semi-solid deformation problem appeared in literature. They primarily concern non-ferrous metals and their alloys [10–45]. The authors of these papers considered a number of aspects related to the deformation of samples with various contents of the liquid and solid phases, starting with equations and computer simulations of heating, and ending with attempts to determine constitutive equations and preliminary computer simulations of deformation of the materials analysed [46–50]. However, there are no solutions concerning the modelling of the steel solidification with its simultaneous plastic deformation.

Choi, in his paper [15], analysed the influence of the holding time of aluminium samples at the last stage of upsetting and selected the optimum holding time on the basis of the final product shape. The experimental research was conducted in laboratory conditions on an MTS (Material Testing Systems) machine, which enabled the maximum load of up to 25 tonnes to be applied, and induction heating of the material tested to be carried out. Cylindrical samples with a diameter of 44 mm and a length of 65 mm, made of the A356 aluminium alloy were used as the input material for the tests. The experiment included the measurement of temperature changes over time. Appropriately arranged thermocouples were applied for the temperature measurements. Computer simulations of the heat transfer between the sample and tools were made with Fourier's transient heat conduction equation using apparent integration with respect to time. Experiments and computer simulations combined with optimisation techniques allowed the authors of the paper [15] to determine the heat transfer coefficients between the sample and tools. The authors of the paper [16], based upon prior experimental research, conducted a series of compression tests of aluminium alloy samples using their original programme SFAC2D with various tool strokes. In the program, a rigid-viscous-plastic model of the body deformed was used for the solid phase skeleton, combined with the solution of Darcy's equation for the liquid phase. Also attempts to determine the constitutive equations were made. Kang, in his studies [23, 24] of the deformation of aluminium alloys in the di-phase range liquid and solid proposed an equation relating to the strain rate, strain degree and the temperature to the fraction of the liquid phase share. Like the authors of the paper [16], for the computer simulation he used a rigid-viscous-plastic model of the body deformed for the solid phase skeleton, combined with the solution of Darcy's equation for the liquid phase. The initial temperature distribution in the volume of the material analysed is a very important factor, which substantially influences the strain and stress state in the deformation process. In research aimed at the computer simulation of such processes, many authors have tried to tackle a number of problems that occur when heating a sample to a desired temperature. The induction heating method was the prevailing method in laboratory conditions [51–56]. Choi and the authors of the study [51] tested the impact of induction heating on the aluminium alloy microstructure. By using various heating variants and implementing a holding stage at a specific temperature when heating, the changes of temperature at the sample centre and its faces were analysed. The experiments, combined with various variants of input and output power, allowed the authors to select the optimal parameters

of induction heating. The authors of the study [55] used the regression method and neural networks to determine the relationship between the conditions of the induction heating process and the solid phase fraction on the basis of the experiment series for the selected aluminium alloys. Parameters such as the holding time at a specific temperature, re-heating after the holding and the time of such re-heating or the power of induction heating significantly influenced the final quality of the obtained samples. The conditions in which they obtained the minimum grain size and the maximum average temperature measured with four thermocouples in the sample volume [55] were the optimum process conditions. Jung dealt with similar issues in his studies [52, 53]. He analysed the influence of heating conditions on obtaining a homogeneous temperature distribution and a uniform structure across the cross-section of a sample. Also the aluminium alloy was analysed. Kang's studies [54] had a similar nature. Based on Jung's experimental findings and the heating curves developed by Jung [52, 53], he carried out computer simulations of induction heating and compared the results with the experimental findings. A commercial programme ANSYS, which enables induction heating combined with complex thermal conditions to be simulated, was used for the simulations. From the perspective of this monograph subject area, the publication [57] turned out to be very interesting. The authors conducted a few series of resistance heating tests of samples made of aluminium alloy A357 in laboratory conditions. They analysed a number of aspects related to the simulation of resistance heating, e.g. the influence of the initial value of the pressure force between the sample and the electrode on the electric conductivity or the influence of the heating power on the final temperature distribution. Most physical parameters that influence the solidification process are strictly related to temperature changes. Temperature fields in most cases are determined using the solution of Fourier's generalised diffusion equation with the finite element method. For the completeness of the solution, Fourier's equation must be complemented with Neumann-Hankel boundary conditions. Material constants, which are necessary for a model of steel deformation in the semi-solid state, in most cases must be determined experimentally. They are functions of temperature associated with the liquid and solid state of aggregation. The results of computer simulation of the temperature changes in the metal solidification process with the full 3D model presented in the paper [58] may be shown as an example. Generally the modified theory of plasticity is used to analyse the flow of metal in which we can distinguish a mushy zone. This classic theory does not cover such effects as irregularity arising from substantial metal porosity or the relationships between the stress and strain states at very high temperatures. Therefore the modelling of the process of semi-solid metal deformation requires supplementing the model with effects related to the behaviour of the material within the temperature range in which the state of aggregation changes. Recently, thermo-mechanical models of porous material deformation have appeared in literature, including a change in the material density within the temperature range specific to the classic plastic working. The paper [59] in which the authors made an attempt at mathematical modelling of the forging process of these materials may serve as an example. In this case the constitutive equation includes the relative

density of the physical continuum referred to a solid material. Also the material state, where its deformation resistance decays, is an important parameter. Applying the formulated constitutive equation to model forging of porous steel rings allowed the authors of the study [59] to obtain good results of the computer simulation that complied with the experiment. The presented approach may be used for the modelling of metal flow in the semi-solid state if one can determine the relationship between strain and stress for the semi-solid and solid material at very high temperatures. The stress state must be computed for the solidified outer layer with a thermo-elastic-plastic model, taking into account the temperature changes of the solidifying steel and the δ/γ transformation. These computations are conducted in line with the variation formulation and after adopting a discretisation specific to the finite element method. A solution like this is presented in the publication [60]. When applying the presented model to the issues discussed, the main problem is a lack of relationship between strain and stress at extra-high temperatures. The problem of determining the stress-strain relationship for a material in the semi-solid state is much more complex than in the case when this material is deformed at lower temperatures and has been plastically deformed before. Solid materials were subjected to comprehensive tests many times in order to determine the stress-strain relationship at increased temperatures. The paper [61] by Wray, who tested carbon steels, may be used as an example. It is much more difficult to model the behaviour of steel and other alloys within the temperature range in which they transform from liquid to solid. As many effects accompany the solidification, it is difficult to determine precisely the plastic and strength properties of the forming semi-solid structure, which changes its density as a result of strain, temperature changes and the δ/γ transformation. The implementation of Gleeble series thermo-mechanical simulators allowed us to conduct appropriate experimental research to determine those parameters. Those simulators are basically the only units, described in literature and available in the market, which allow similar tests to be performed. Examples of tests with Gleeble simulators are presented by the authors of the papers [62–64], who analysed the conducted experiments with deforming nickel and aluminium alloys. They showed that not only changes in the dependence of stress on strain were very strongly related to temperature, but also depended on the cooling rate within the temperature range between the liquidus and solidus lines. The papers [63, 64] also reveal a linear dependence of the stress causing material destruction on the size of grain which forms during the material solidification. Other than at lower temperatures, for an equiaxial structure the stress causing material destruction is directly proportional to the grain size [63]. The authors explain this effect by the melting of grain boundaries. It results in the need to track changes in the size of the forming grain. During the solidification, the material changes its state of aggregation and at a certain temperature it becomes mechanically strong. Even though it is believed [65] that at increased temperatures the carbon content in steel has a minimal impact on its deformation resistance, it influences the nil strength temperature [66]. For low carbon steels, the material shows some deformation resistance even at a 60% fraction of the solid phase. High carbon steels recover their strength only at a solid phase fraction over 80%. However, the material is brittle and

its temperature must decrease so that it can be deformed. Generally, it is believed that although the temperature at which the material loses its strength depends on the carbon content in the steel, the solidifying material becomes plastic at the temperature at which the solid phase fraction is about 98% and its dependence on the percentage of carbon is minimal. The authors of the article [66], when carbon steel properties were tested, found that the plastic behaviour of low and high carbon steels differs at very high temperatures. They tested a low (0.12%C), a medium (0.41%C) and a high carbon steel (0.81%C). They found that these steels recovered their tensile strengths at temperatures of 1505, 1455 and 1404 °C respectively, and the increase in this strength along with the decrease in temperature had a similar nature, close to linear. However, these steels demonstrated different behaviour regarding ductility changes when cooled. Medium and high carbon steels recovered their ductility at temperatures of 1374 and 1314 °C, and showed a substantial increase in their ductility when the temperature decreased. Low carbon steels recovered slight ductility at a temperature higher than other steels. For instance, for steel containing 0.12%C the temperature of ductility recovery was 1475 °C. Yet initially the increase in ductility was slow. A faster growth in the ductility of this steel was only observed at a temperature of 1438 °C. This effect was caused by the occurring δ/γ transformation, which started during the solidification at a temperature of 1486 °C, and ended below the solidus line exactly at 1438 °C. A local decrease of the specific volume of steel as a result of the δ/γ transformation causes a strain, which when superimposed on the thermal strain causes the possibility of faster cracking and is the reason for a decrease in the material ductility. Below the transformation temperature the low carbon steel demonstrates a rapid increase in its ductility. The paper [66] also presents a quantitative description of the changes of the parameters discussed. The authors presented a number of relationships which allow the critical stress, i.e. the point at which cracks appear in the steel, to be determined. They showed that the dependence of the yield stress on the temperature and strain rate may be described with the following relationship:

$$\dot{\epsilon}_p = A \exp\left(-\frac{Q}{RT}\right) (\sinh(\alpha\sigma))^{\frac{1}{m}} \quad (2.1)$$

where:

$\dot{\epsilon}_p$ —plastic deformation rate,

T —absolute temperature,

σ —yield stress,

Q —plastic deformation process activation energy,

R —gas constant,

A, α, m —material constants.

The authors [66, 67] described the critical stress to initiate a crack within the range in which phases γ and δ coexist with the following formula:

$$\varepsilon_c = \left(\frac{\varphi}{\dot{\varepsilon}_p^m \Delta T_B^n} \right) \quad (2.2)$$

where:

$\dot{\varepsilon}_p$ —plastic deformation rate,

φ, m, n —material constants,

ΔT_B —the temperature range of reduced ductility.

On the basis of the quoted papers one may conclude that despite serious experimental difficulties, the application of the foregoing mathematical formalism to describe the mechanical properties of the material in the semi-solid state gives very good results. It needs to be stressed that the research quoted in the papers [66, 67] was made with an old type of Gleeble simulator.

There are many papers concerning the determination of strain-stress curves in the available literature, largely for non-ferrous metals [66, 68–76]. In recent years also, attempts to describe similar relationships for steels and attempts to deform in the semi-solid state have appeared [46–50, 67, 77–92]. The main reason for the numerous tests and the determination of constitutive equations for non-ferrous metals is the fact that the liquidus and solidus temperatures for non-ferrous metals are lower than for steels. This fact allowed preliminary tests to be conducted, usually in laboratory conditions, in which samples were melted and deformed slowly. On the basis of test results computer simulations were conducted to verify the findings. When Gleeble simulators were implemented, the technical and research possibilities increased. Whereas the development of continuous steel casting practices in recent years has been very intensive, the research work in this field carried out with new units may constitute the research foundation for the development of new practices. In most papers, to describe changes of stress as a function of strain, the authors used equations combining the strain rate, strain degree and temperature. The fraction of the solid or liquid phase was an additional parameter taken into account in the equations. Kang's studies [23, 24] may be used as an example. He described the dependence of the yield stress on the temperature and strain rate with the following relationship:

$$\sigma = K \dot{\varepsilon}^m \exp\left(\frac{Q}{RT}\right) (1 - \beta f_l)^{\frac{2}{3}} \quad (2.3)$$

where:

K, m —material constants,

β —equilibrium factor,

T —absolute temperature,

β —equilibrium factor,

Q —plastic deformation process activation energy,

f_l —liquid phase fraction.

The curves were determined on the basis of compression tests, at a 50% fraction of the liquid phase and small strain rates under 1 s^{-1} . The obtained dependences became the basis for procedures simulating the deformation of aluminium alloys in the semi-solid state. In his study [71] Kopp conducted a series of compression tests of samples made of the Sn-15%Pb alloy for two variants with the solid phase fraction of 0.55 and 0.65. On the basis of the conducted tests, the strain-stress curves were determined. Using the commercial FEM software, they made a series of computer simulations for various parameters of the constitutive model. The conducted simulations allowed them to evaluate the formulated constitutive model. The evaluation included a comparison of force parameters obtained during the experiment and by computer simulation, where good compliance of the analysed parameters was obtained.

Other examples may be found in papers [68–70, 72–74, 76, 79, 80, 83, 91, 93–96] concerning primarily non-ferrous metals. A paper by Lewandowski deserves attention [73], where the author presents a number of aspects related to the compression test modelling and determining flow curves for the aluminium alloy 718. Deformation experiments were conducted at very low strain rates of 0.001 s^{-1} . Tests on steels were published in the following papers: [67, 79, 80, 91]. Tseng in his study [91], like Lewandowski in his [73], presented a number of aspects related to the compression test modelling and determining strain-stress curves for the selected carbon steels. By analysing the impact of the solid phase content, he conducted a few series of deformation tests at low speeds ($<0.012 \text{ s}^{-1}$) and obtained curves for various fractions of the solid phase in the sample volume. In publication [67] the authors presented their findings concerning the determination of flow curves for steels in the temperature range between 1100 and 1450 °C. Experimental work was conducted to determine the impact of the temperature and strain rate on the plastic behaviour of two types of carbon steel. The first one containing 0.137% of carbon was subjected to tensile tests at temperatures of 1100, 1200 and 1300 °C and was used for determining flow curves for austenite. In order to examine similar relationships for ferrite δ , a steel containing 0.0026% of carbon was selected and was deformed at temperatures of 1400 and 1450 °C. The tests were conducted with a Gleeble simulator. The authors proved the full suitability of Garofalo's model [97] modified by Han to describe the flow curves of the tested steels, dependent on the temperature and strain rate:

$$\dot{\varepsilon}_p = A \exp\left(-\frac{Q}{RT}\right) (\sinh(\beta K))^{\frac{1}{m}} \quad (2.4)$$

$$\sigma = K \varepsilon^n \quad (2.5)$$

where:

$\dot{\varepsilon}_p$ —plastic deformation rate,

T —absolute temperature,

σ —yield stress,

Q —plastic deformation process activation energy,

K —strenght coefficient,

n —strain hardening exponent,

A, β, m —material constants.

The steels were tested at very high temperatures. This model was used to analyse the deformation of porous materials at lower temperatures, not exceeding 1200 °C and showed its full suitability [59]. The Han relationship can also serve as the basis for the constitutive equation for high temperatures. In paper [67], very good compliance of the obtained experimental findings with the values computed with this model was shown. However, the main objective of the authors was to investigate flow curves for strain rates from 0.0001 to 0.01 s⁻¹ and very small plastic deformations, not exceeding 0.1. For the cases of plastic deformation of semi-solid steel, experimental research should be conducted to determine the material constants for a much broader range of strains and strain rates. One of the most topical publications is Jing's paper [80] concerning primarily the determination of flow curves for steel 304. The curves were determined on the basis of compression tests. The liquidus and solidus temperatures were 1450 and 1390 °C respectively. The deformation temperature range for samples with a diameter of 12 mm and a height of 12 mm was between these two temperatures. During the experiment, the force and the base elongation of the sample were measured, as well as the temperatures read from the thermocouple indications. At the first stage the sample was heated to the deformation temperature within the range between the liquidus and solidus lines according to a set temperature schedule. At the final stage it was deformed at strain rates from 0.5 to 10 s⁻¹.

The tests carried out by the authors of the papers [67, 79, 80, 91] may constitute the research foundation for modelling and designing new continuous steel casting practices. To be competitive in the market one should aim at obtaining products with consistent and good quality. Unfortunately, steel tests at very high temperatures are still very expensive. For business and technological reasons they cannot be conducted under industrial conditions. The Gleeble simulators and computer tomographs (CT scanners), more and more widely available, may provide an alternative. A Gleeble 3800 simulator enables the steel continuous casting process to be physically simulated. The main purpose of the simulation is to use a small sample to reconstruct the changes of temperature, strain and stress that the material undergoes in the industrial process. The evaluation of the mechanical properties of samples subjected to various simulation variants provides the basis for developing the so-called “casting map”, which enables the optimal parameters of the continuous caster operation when casting a specific steel grade to be determined. In practice, time-temperature-reduction (TTR) diagrams similar to TTT diagrams are constructed. These diagrams show areas with a limited ductility, and a thorough knowledge of those areas allows us to adjust the casting process parameters, such as for instance the casting speed, so as to avoid the potential threat of cracks in the strand. The Gleeble simulator provides a rare—from an experimental point of view—opportunity to combine the simulation of continuous casting with the plastic

deformation applied during or immediately after the solidification of the working part of the sample. In both processes, i.e. the solidification and the plastic deformation, in order to determine the impact of process parameters on the microstructural changes, the sample may be cooled with gas (argon, compressed air), a water and air mixture, or water, or cooled with a rate typical of the simulated production process. Increasing availability of modern equipment, such as computer tomographs, allows the medium tested to be analysed without destroying it. The analysis of the remelting zone and the ability to make a virtual cross-section for determining the area of the formed porous zone (Fig. 2.1), or the possibility of the 3D separation of the whole porous zone (Fig. 2.2) are examples from the original research of the author.

Additionally, thanks to the use of specialist dedicated software to analyse the findings, results and information, impossible with other methods, can be obtained. The obtained findings may be the basis for the verification of the adopted model assumptions in the context of numerical modelling. Examples of the application of the computer tomography in high-temperature research are shown in papers [88, 98–102]. The authors of [88] used the tomographic analysis method to directly analyse the deformation zone of a steel sample deformed with a solid phase fraction of 55–65%. On the other hand, the paper by [100] is very interesting from the perspective of this monograph. The scope of the performed tests covered physical simulations with a Gleeble 3500 simulator and numerical simulations of the deformation of an Al–Cu alloy. Everything was complemented by methodology aided by the computer tomography for determining the function describing changes in stress versus strain, strain rate and temperature. To describe, the authors used the following equation form [100].

Fig. 2.1 A virtual cross-section of a sample with a visible porous zone (author's original research, carbon steel)

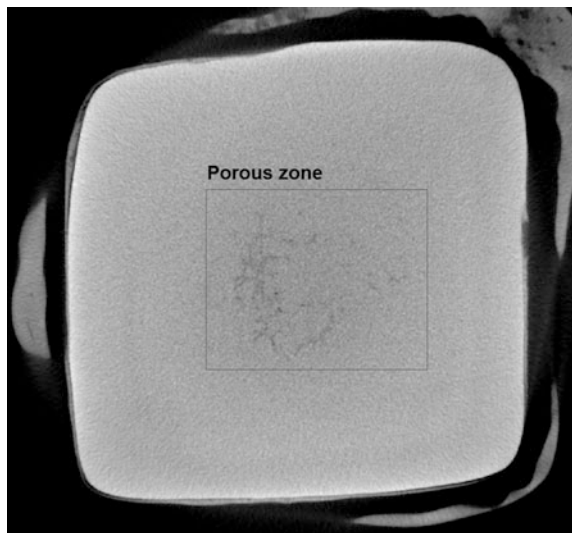
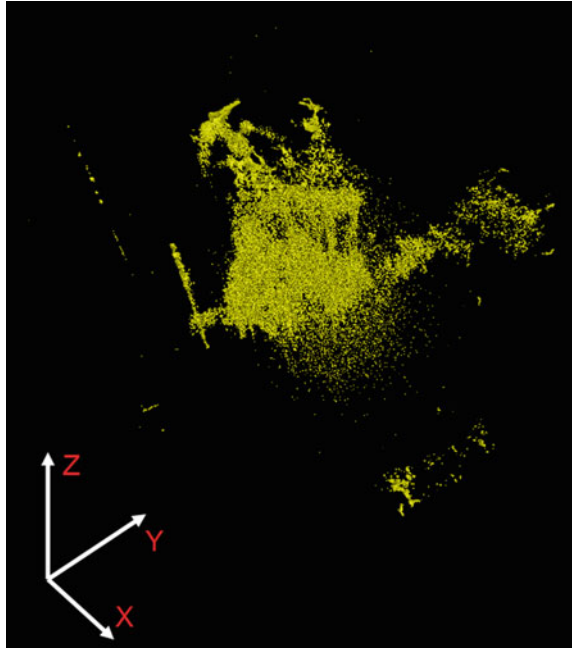


Fig. 2.2 A 3D view of a separated porous zone (author's original research, carbon steel)



$$\sigma(\varepsilon, \dot{\varepsilon}, T) = K(\varepsilon, \dot{\varepsilon}, T) \varepsilon^{m(T)} \dot{\varepsilon}^{n(T)} \quad (2.6)$$

where σ is the stress, ε is the plastic strain, $\dot{\varepsilon}$ is the strain rate, K is the flow stress coefficient, m is the strain hardening factor and n is the strain rate sensitivity factor.

The development of the continuous casting practice, in particular of the twin-roll strip casting process, which is the most important for the industry, continues [103–122]. The development of the continuous casting practice is focused on the manufacturing of near net shape products. This tendency is conditioned by business considerations and competition in the market, and indirectly obviously by advantageous environmental impact. Many factors influence the internal state of the strip cast in the continuous process. The most important are: the degree of superheating, casting speed, characteristics of heat flow between the solidifying shell and the rolls, characteristics of the flow of the liquid metal feeding the mould [123]. Physical conditions, in which the cast strand solidification process occurs, very strongly determine its future state, including such features as the share of individual crystalline zones, the distance between dendrite branches, the austenite grain size, microsegregation and macrosegregation degree, and also the type and arrangement of cracks, or the level of internal stress. These features significantly influence the product quality. Therefore, they must be controlled by the appropriate selection of process parameters, and by the impact on the liquid steel during the process. By focusing on the secondary cooling zone effects, vital for the formation of the cast strand quality parameters, one can find that—from a mechanical point of view, and

also due to the heat flow nature—it is the most complex stage of the process. Within a cast strand we can distinguish the solidified outer layer (shell), the partially solidified mushy zone and the central liquid area, which are characterised by diversified physico-chemical properties. In these conditions the plastic behaviour of the medium considerably differs from the one that is commonly observed, for instance in the hot working processes. The prerequisite for numerical simulations of the changes in the temperature field and stress in a cast strand is to have functions describing the dependence of the thermophysical constants on temperature and the stress-strain relationship for diversified strain conditions. Without this data the numerical simulation of the casting and rolling process cannot be conducted with sufficient accuracy. In this case, it is necessary to apply a simplified approach to continuous casting physical simulation problems—to set linear functions of temperature changes versus time—developed approximately on the basis of temperature measurements carried out at continuous casting facilities [90].

In recent years many companies worked on the development of the rolling process with a semi-solid core. Whilst thin strip casting combined with subsequent rolling is a simple, improved method of the conventional rolling process, rolling a strip, in which both the solid and the liquid phases coexist, is a new process. Cold rolling following simple strand casting is a long process and it is not cost-effective because of energy reasons. For the technological reasons the process should be developed to simplify or eliminate some operations, which would drastically reduce the energy costs. It also involves beneficial environmental impact, due to the reduction of gas emissions. Processes of casting immediately followed by rolling have various versions, which depend on the applying companies and differ with details of industrial installations. A few concepts have been developed by such companies as SMS Demag AG, VAI (Voest Alpine) or Tippins Incorporated. The selected installations include [124]:

- CSP (Compact Strip Production),
- LCR (Liquid Core Reduction),
- ISP (Inline Strip Production),
- AST (Arvedi Steel Technology),
- CONROLL (CONtinuous thin casting ROLLing Technology),
- TSP (Tippins Samsung Process),
- CONROLL (CONtinuous thin casting ROLLing Technology),
- CPR (Casting Pressure Rolling),
- DSC (Direct Strip Casting),
- “Danieli” (Thin slab caster),
- QSP (Quality Strip Production),
- UTHS (Ultra Thin Hot-Strip),
- SMI (Sumitomo heavy industries and Mitsubishi heavy Industries),
- ESP (Endless Strip Production).

Continued development of new technologies or their modification forces designers to seek new solutions that will support decision-making processes at each

project stage. The development of advanced physical simulation tools as well as numerical methods, which due to long calculation times could not have been used formerly in course of design work, enables the analysis of processes both from the standpoint of continuous media mechanics, fluid mechanics or high-pressure phenomena. This is a common characteristic of the three technological processes presented in the diagrams (Figs. 2.3, 2.4 and 2.5), with respect to which the author of the present monograph conducts advanced experimental and model studies. As mentioned earlier, the dominant continuous medium analysis method is the finite element method (FEM). In terms of fluid flow analysis or analyses of solidification in conjunction with flow in the solidifying solid phase, the smooth particle hydrodynamics method (SPH) gains importance [125].

The SPH method was first developed by [126, 127] to solve astrophysical problems in a three dimensional open space. In recent years, considerable progress in the development of solutions using meshless methods has been achieved, enabling phenomena occurring in many areas, including the description of metallurgical processes such as solidification [128], to be simulated. In many cases, both in industry and science, the issues concern fluid mechanics. The scale of the phenomena studied is very wide, from micro- through meso-, ending at the macro-level. With this approach, it is possible to consider many interesting phenomena that occur at the connection of scales, such as multiphase flows [129] or a turbulent flow [130]. One of the most commonly used methods for simulating the behaviour of fluids and their flow is called the particle method. Smoothed Particle Hydrodynamics (SPH) is a method of this type. In the SPH method [126], the Lagrangian approach is applied to describe the fluid, where calculation points move together with the flowing liquid as opposed to Euler's approach, wherein the calculation points do not change their positions. Simulation of the behaviour of real fluids using computer modelling is of great importance both for industry [131] and

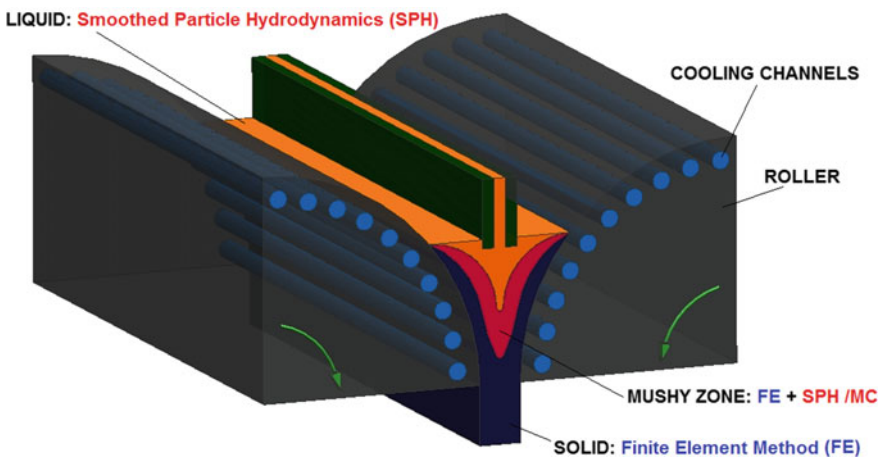


Fig. 2.3 The scheme of direct strip casting process (DSC)

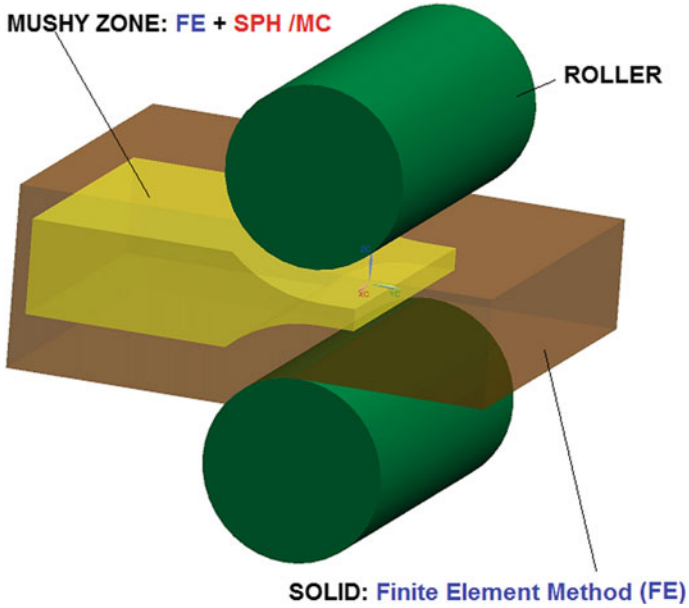


Fig. 2.4 The scheme of soft-reduction process (SR)

LIQUID: Smoothed Particle Hydrodynamics (SPH)

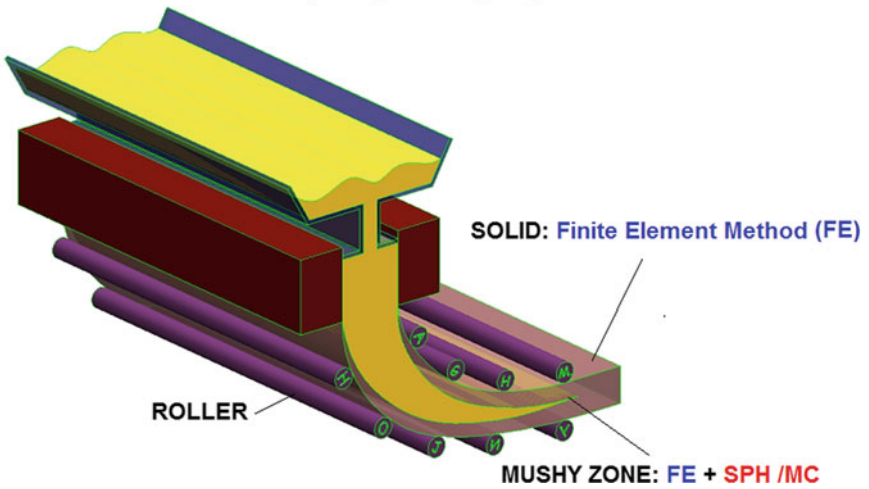


Fig. 2.5 The scheme of continuous casting and rolling process (CCR)

for the development of science in many fields. Research is being conducted on the use of the SPH method to simulate many industrial processes such as: forecasting the metal flow in the process of high-pressure casting of components for the

automotive industry [132], aviation [133], as well as the power sector [123]. Another example is the use of the SPH method using commercial software like LS-DYNA to simulate the aluminium flow in a foundry mould [134, 135]. A description of the behaviour of fluids, including multiphase fluids, is extremely important for many technical applications, including those in the metal industry. Such models should take into account the complexity of the simulated systems. Due to their complex nature, systems of this type can cause many problems with the proper simulation of thermodynamic parameters, and the assumption of an adequate flow in systems of vessels with complex shapes. The interesting, and yet at the same time complicated behaviour of fluids is primarily due to the interaction processes. The SPH method, thanks to its high flexibility, is widely used not only for modelling flows (including multiphase) of the liquid, but also to describe the behaviour of solids—heat conductivity, or problems accompanying explosions. Modern models of fluids, which allow the issues concerned to be simulated with acceptable accuracy, due to their high complexity are difficult to design and implement. The use of modern computer architecture and customised algorithms is required to obtain reasonable computing time to enable these methods to be useful. The authors of the publication [86] presented the application of the SPH method to simulate the solidification process. The research was conducted for a single-component fluid and a two-component mixture. After verification of the results for the case of a single-component alloy, an attempt to simulate a two-component alloy was made. The simulation results were verified with the experiment. The SPH method is also used for the modelling of deformation processes such as metal forging, where large deformation of the material occurs, causing serious problems in using mesh methods like the Finite Element Method (FEM). The authors of the publication [136] indicated that the SPH was a useful simulation method that allowed them to obtain information on the deformable material and the flow of material while forging real industrial components. Through the simulation process, the quality of the final product and the impact of process parameters and material properties were established. Also the force needed to sufficiently fill the mould cavity and the effect of the hardening material, which gives the final product its quality, were defined. The method also allowed the prediction of defects such as failure to fill the forging die. The SPH method can thus also be potentially used to assess the quality of forged products.

The authors of the publication [137] successfully applied the SPH method to simulate the fluid flow in an isotropic porous material. The porous structure is defined in the mesoscopic scale by randomly assigning some particles with fixed positions. The designated flow field, calculated at a steady state of the two-dimensional isotropic system, provides information on the macroscopic fluid flow. Meshless methods are widely used in modelling problems with a large deformation or a loss of material cohesion. In the publication [138], the authors use the SPH method to present a model of material cutting. Preliminary studies for the two-dimensional model have shown the suitability of the method to correctly estimate shear forces, as shown in several examples of the perpendicular cut. Finally, the modelling of cutting forces in a three-dimensional space was

performed. In many cases of simulations of complex physical processes, it is reasonable to apply a hybrid method combining the Finite Element Method and meshless methods. To combine both methods, it is required to determine the interactions between the models. The authors of the publication [139] describe several methods of interaction and their combinations in order to obtain satisfactory results. The discussion on the interaction between Lagrangian elements and the particles of the SPH method was included. Sample calculations and the usage of appropriate algorithms were exemplified by a commercial program. In the paper [140], an overview of methods allowing the coupling of the meshless methods with the Finite Element Method was presented. One of them is the coupled master-slave type, wherein the particles are associated with the nodes of the finite element mesh. The coupling, through the interaction of particles with the nodes of the element mesh and vice versa, is satisfactory. Finally, many static and dynamic problems were tested, comparing the results to the experimental data. Another example of coupling of the Finite Element Method with a meshless method is studying the structural resistance to destruction. In the publication [141], to verify the established thesis, the problem of the hydrostatic pressure simulation was also considered. Taking into account the wide use of the SPH method to model phenomena in many fields including metallurgical processes, it is possible to determine the flow of material during the solidification of a slab manufactured in the continuous casting process. Alternative numerical methods used presently in engineering practice spanning, among others, solidification simulations, are for instance, cellular automata (CA) and the Monte Carlo (MC) method. Approaches to modelling of effects accompanying the solidification with the use of cellular automata method, known from the literature, are fairly diverse and elaborated [142, 143]. The first group of models focuses on microstructure details, including the simulation of single dendritic grains, with the accuracy of at least to the second order branches [43]. The second group of models deals with the grain growth kinetics, and not its shape, which is assumed in advance. The best known model of this type was created by Rappaz and Gandin [144–147]. It was assumed in the algorithm that the grain envelope is a square (a regular octahedron for 3D areas), which is better satisfied when the so-called incubation time of second order branches is shorter. It is possible to present various crystallographic grain orientation by a change in the square position (regular octahedron for 3D areas), with respect to the cellular automata mesh. Models that map the relevant effects primarily quantitatively constitute the last group of models. The transition rules used in these models do not have an explicit physical interpretation, and their main task is to reconstruct the branched structure of dendritic grains. A Brown and Brucet paper [148] is an interesting example. The paper deals with the modelling of three-dimensional dendritic grains of pure metal. Single grains are considered during their free growth in an undercooled liquid. Each cell of the three-dimensional cellular automaton has its temperature and state 1 or 0 assigned, depending on whether the cell belongs to the solid or the liquid phase, respectively. The solid state appears in those cells which have an adequate number of solidified neighbours, and their temperature is below the critical temperature (depending on the number of the solidified neighbours). The

effect of the latent heat liberation is presented by increasing the temperature of the solidifying cell to a certain, set value corresponding to the solidification temperature. The heat flow in the area is executed with the following procedure: the average temperature of the six closest neighbours is calculated (von Neumann neighbourhood), and then the temperature of a specific cell is changed towards this average temperature by a value depending on the heat transfer coefficient.

A further method that had gained popularity in recent years is the Monte Carlo method [87, 149, 150]. The use of this method is very broad, beginning from uses in biology and medicine [151], all the way to welding processes [152–155], in which analysed are also phenomena such as e.g. granulation growth during solidification or the growth of granularity in the heat influence zone [150, 156–161]. Continued development of computer equipment in terms of processing speed, including the possibility of use of GPU for calculations creates the perfect base for the design and implementation of fully 3D models basing on this method. On the other hand, the shape of the mixed zone itself (Figs. 2.3, 2.4 and 2.5) is often irregular, and this also determines the choice and use of numeric solutions basing on full spatial solutions.

The conducted analysis of literature indicates a lack of comprehensive methodology (from the physical and numerical side) supporting the design of new high-temperature technologies and the analysis of selected phenomena/parameters that would accompany it. However, the need of controlled rolling of cast strands is pointed out. Therefore, the results of a computer simulation or physical simulation of the analysed process will be useful to control the process parameters. Creating the modelling concept integrating the physical and computer simulation areas with simultaneous full or partial information exchange between those areas is pioneering in terms of theory.

References

1. Glowacki M (2005) The mathematical modelling of thermo-mechanical processing of steel during multi-pass shape rolling. *J Mat Proc Tech* 168:336–343
2. Lenard JG, Pietrzyk M, Cser L (1999) *Mathematical and physical simulation of the properties of hot rolled products*. Elsevier, Amsterdam
3. Pietrzyk M, Lenard JG (1991) *Thermal mechanical modelling of the flat rolling process*. Springer-Verlag, Berlin
4. Glowacki M (1995) Modelling of heat transfer, plastic flow and microstructural evolution during shape rolling. *J Mat Proc Tech* 53:159–166
5. Glowacki M (1996) Simulation of rail rolling using the generalized plane-strain finite-element approach. *J Mat Proc Tech* 62:229–234
6. Glowacki M (1998) Termomechaniczno-mikrostrukturalny model walcowania w wykrojach kształtowych. AGH, Krakow
7. Glowacki M (1996) Finite element three-dimensional modelling of the solidification of a metal forming charge. *J Mat Proc Tech* 60:501–504
8. Pietrzyk M (1992) *Metody numeryczne w przerobce plastycznej metali*. AGH, Krakow

9. Siska P, Hojny M (2002) Computer simulation of influence of lubricant on cold drawing process of steel wire from material 11320. In: Proceedings of COMATECH, Trnava
10. Aashuri H (2005) Globular structure of ZA27 alloy by thermomechanical and semi-solid treatment. *Mat Sci Eng* 391:77–85
11. Ahmed SG (2005) An approximate method for evaporation problem with mushy zone. *Eng Analysis Bound Elem* 29:161–165
12. Chen CP, Tsao C (1997) Semi-solid deformation of non-dendritic structures phenomenological behavior. *Acta Mater* 45:1955–1968
13. Chen YN, Wei JF, Zhao YQ (2009) Compressive deformation and forging behavior of Ti14 alloy in semi-solid state. *Mat Sci Eng* 520:16–22
14. Choi JC, Park JH, Kim BM (2000) Finite element analysis of the combined extrusion of semi-solid material and its experimental verification. *J Mat Proc Tech* 105:49–54
15. Choi JC, Park JH, Lee BK (1998) Finite element analysis of compression holding step in semi-solid forging and experimental confirmation. *J Mat Proc Tech* 81:450–457
16. Dae CK, Gyu SM, Byung MK et al (2000) Finite element analysis for the semi-solid state forming of aluminium alloy considering induction heating. *J Mat Proc Tech* 100:95–104
17. Eskin DG, Suyitno L (2004) Mechanical properties in the semi-solid state and hot tearing of aluminium alloys. *Prog Mat Sci* 5:629–711
18. Gang C, Fengyu L, Shengjie Y et al (2016) Constitutive behavior of aluminum alloy in a wide temperature range from warm to semi-solid regions. *J Alloy Compd* 674:26–36
19. Haghayeghi R, Zoqui EJ, Halvae A (2005) An investigation on semi-solid Al-7Si-0.3 Mg alloy produced by mechanical stirring. *J Mat Proc Tech* 169:382–387
20. Hong Y, Bingfen Z (2006) Thixotropic deformation behavior of semi-solid AZ61 magnesium alloy during compression process. *Mat Sci Eng* 132:179–182
21. Hosseini Yekta F, Sadough Vanini SA (2015) Simulation the flow of semi-solid steel alloy using an enhanced model. *Met Mater Int* 21:913–922
22. Hwang JH, Ko DC, Min GS et al (2000) Finite element simulation and experiment for extrusion of semi-solid Al 2024. *Int J Mach Tools Man* 40:1311–1328
23. Kang CG, Jung HK (1999) Finite element analysis with deformation behavior modeling of globular microstructure in forming process of semi-solid materials. *Int J MechSci* 41:1423–1445
24. Kang CG, Kang BS, Kim JI (1998) An investigation of the mushy state forging process by the finite element method. *J Mat Proc Tech* 81:444–449
25. Kang CG, Yoon JH (1997) A finite-element analysis on the upsetting process of semi-solid aluminum material. *J Mat Proc Tech* 66:76–84
26. Kang CG, Choi JS, Kim KH (1999) The effect of strain rate on macroscopic behavior in the compression forming of semi-solid aluminum alloy. *J Mat Proc Tech* 88:159–168
27. Kang CG, Jung YJ, Youn SW (2003) Horizontal reheating of aluminum alloys and semi-solid casting for a near net shape compressor component. *J Mat Proc Tech* 135:158–171
28. Khosravi H, Eslami-Farsani R, Askari-Paykani M (2014) Modeling and optimization of cooling slope process parameters for semi-solid casting of A356 Al alloy. *Trans Nonferr Met Soc China* 24:961–968
29. Koc M, Vazquez V, Witulski T et al (1996) Application of the finite element method to predict material flow and defects in the semi-solid forging of A356 aluminum alloys. *J Mat Proc Tech* 59:106–112
30. Lapkowski W, Sinczak J, Ruzs S (1997) Feasibility of metal forming in semi-liquid state. *J Mat Proc Tech* 63:260–264
31. Lashkari O, Ghomashchi R (2008) Deformation behavior of semi-solid A356 Al-Si alloy at low shear rates: effect of fraction solid. *Mater Sci Eng, A* 486:333–340
32. Lu Y, Li M, Huang W et al (2005) Deformation behavior and microstructural evolution during the semi-solid compression of Al-4 Cu-Mg alloy. *Mat Char* 54:423–430
33. Martin CL, Favier D, Suery M (1999) Fracture behaviour in tension of viscoplastic porous metallic materials saturated with liquid. *Int J Plast* 15:981–1008

34. Prabhu TR (2016) Microstructure and mechanical properties of a thixoforged (semi solid state forged) Al–Cu–Mg alloy. *Arch Civ Mech Eng* 16:335–343
35. Rongfu X, Xuelei T (2014) Tensile properties of the semi-solid state in solidifying aluminum alloys. *Russian J Nonferr Met* 55:443–449
36. Seo PK, Youn SW, Kang CG (2002) The effect of test specimen size and strain-rate on liquid segregation in deformation behavior of mushy state material. *J Mat Proc Tech* 131:551–557
37. Shiomi M, Takano D, Osakada K et al (2003) Forming of aluminium alloy at temperatures just below melting point. *Int J Mach Tools Man* 43:229–235
38. Yongnan CH, Chuang L, Fengying Z et al (2015) Effect of temperature on segregation and deformation mechanism of α + Ti2Cu alloy during semi-solid forging. *Rare Met Mater Eng* 44:1369–1373
39. Yoon HJ, Im YT (2001) Finite element modeling of the deformation behavior of semi-solid materials. *J Mat Proc Tech* 113:153–159
40. Wang JJ, Phillion AB, Lu GM (2014) Development of a visco-plastic constitutive modeling for thixoforging. *J Alloy Compd* 609:290–295
41. Zhao YQ, Wu WL, Chang H (2006) Research on microstructure and mechanical properties of a new α + Ti2Cu alloy after semi-solid deformation. *Mat Sci Eng* 416:181–186
42. Zhu Y, Tang J, Xiong Y et al (2001) The influences of the microstructure morphology of A356 alloy on its rheological behavior in the semi-solid state. *Sci Tech Adv Mat* 2:219–223
43. Zhu MF, Hong CP (2001) A modified cellular automaton model for the simulation of dendritic growth in solidification of alloys. *ISIJ Inter* 41:436–445
44. Zu L, Luo S (2001) Study on the powder mixing and semi-solid extrusion forming process of SiCp/2024Al composites. *J Mat Proc Tech* 114:189–193
45. Kirkwood DH, Suéry M, Kapranos P et al (2010) Semi-solid processing of alloys. Springer Series in Materials Science, Springer, Heidelberg
46. Cuiqing Z, Renbo S (2014) Evolution of microstructure and mechanical properties for 9Cr18 stainless steel during thixoforging. *Mater Des* 59:502–508
47. Favier V, Atkinson HV (2011) Micromechanical modelling of the elastic-viscoplastic response of metallic alloys under rapid compression in the semi-solid state. *Acta Mater* 59:1271–1280
48. Macioł P, Zalecki W, Kuziak R (2010) Results of experimental investigations of tool steel during forming in semi-solid state. *Int J Mater Form* 3:759–762
49. Phillion AB, Cockcroft SL, Lee PD (2008) A three-phase simulation of the effect of microstructural features on semi-solid tensile deformation. *Acta Mater* 56:4328–4338
50. Sistaninia M, Phillion AB, Drezet JM et al (2011) Simulation of semi-solid material mechanical behavior using a combined discrete/finite element method. *Metall Mater Trans A* 42:239–248
51. Choi JC, Park JH, Kim BM (1999) The influence of induction heating on the microstructure of A356 for semi-solid forging. *J Mat Proc Tech* 87:46–52
52. Jung HK, Kang CG (2002) Induction heating process of an Al–Si aluminum alloy for semi-solid die casting and its resulting microstructure. *J Mat Proc Tech* 120:355–364
53. Jung HK, Kang CG (2000) Reheating process of cast and wrought aluminum alloys for thixoforging and their globularization mechanism. *J Mat Proc Tech* 104:244–253
54. Kang CG, Seo PK, Jung HK (2003) Numerical analysis by new proposed coil design method in induction heating process for semi-solid forming and its experimental verification with globalization evaluation. *Mat Sci Eng* 341:121–138
55. Park JH, Choi JC, Kim YH et al (2002) A study of the optimum process for A356 Alloy in semi-solid forging. *Int J Adv Man Tech* 20:277–283
56. Sang YL, Jung HL, Young SL (2001) Characterization of Al 7075 alloys after cold working and heating in the semi-solid temperature range. *J Mat Proc Tech* 111:42–47
57. Seiji M (2002) Application of resistance heating technique to mushy state forming of aluminium alloy. *J Mat Proc Tech* 126:477–482

58. Malinowski Z, Glowacki M, Pietrzyk M (1994) Finite element method in application to 3-D problems: simulation of the heating of slabs. *Arch Met* 39:278–294
59. Han HN, Lee Y, Oh KH et al (1996) Analysis of hot forging of porous metals. *J Mat Sci Eng* 206:81–89
60. Dudek K, Glowacki M, Pietrzyk M (2000) Modelling of stress generated in steels by phase transformation. In: *Proceedings of. Modellierung von Prozessen der Stahlerzeugung und Stahlverarbeitung, Freiberg*
61. Wray PJ (1982) Effect of carbon content on the plastic flow of plain carbon steels at elevated temperatures. *Metall Trans* 13A:125–134
62. Lin CS, Sekhar JA (1993) Semi-solid deformation in multi-component nickelaluminum—directionally solidified alloys. *J Mat Sci* 28:3581–3588
63. Lin CS, Sekhar JA (1994) Solidification morphology and semi-solid deformation in superalloy Rene 108—equiaxed solidified microstructures. *J Mat Sci* 29:3637–3642
64. Lin CS, Sekhar JA (1994) Solidification morphology and semi-solid deformation in superalloy Rene 108—directionally solidified alloys. *J Mat Sci* 29:5005–5013
65. Wolf M, Kurz M (1981) The effect of the carbon content on solidification of steel in the continuous casting mold. *Metall Trans* 12B:88–93
66. Seol DJ, Won YM, Yeo T et al (2000) Mechanical behaviour of carbon steels in the temperature range of mushy zone. *ISIJ Int* 40:356–363
67. Seol DJ, Won YM, Yeo T et al (1999) High temperature deformation behaviour of carbon steel in the austenite and δ -ferrite regions. *ISIJ Int* 39:91–98
68. Bigot R, Favier V, Rouff C (2005) Characterisation of semi-solid material mechanical behaviour by indentation test. *J Mat Proc Tech* 160:43–53
69. Ferrante M, Freitas E (1999) Rheology and microstructural development of a Al-4wt% Cu alloy in the semi-solid state. *Mat Sci Eng* 27:172–180
70. Haafte WM, Kool W, Katgerman L (2002) Tensile behaviour of semi-solid industrial aluminium alloys AA3104 and AA5182. *Mat Sci Eng A336*:1–6
71. Kopp R, Choi J, Neudenberger D (2003) Simple compression test and simulation of an Sn-15% Pb alloy in the semi-solid state. *J Mat Proc Tech* 135:317–323
72. Lapkowski W, Pietrzyk M, Sinczak J (1992) Behaviour of metal alloys during plastic deformation in partly liquid state. *J Mat Proc Tech* 34:481–488
73. Lewandowski MS, Overfelt RA (1999) High temperature deformation behavior of solid and semi-solid alloy 718. *Acta Mat* 47:4695–4710
74. Martin L, Braccini M, Suery M (2002) Rheological behavior of the mushy zone at small strains. *Mat Sci Eng A325*:292–301
75. Rokni MR, Zarei-Hanzaki A, Roostaei AA et al (2011) Constitutive base analysis of a 7075 aluminum alloy during hot compression testing. *Mater Des* 32:4955–4960
76. Sigworth GK (1996) Rheological properties of metal alloys in the semi-solid state. *Can Metall Q* 35:101–122
77. Hosseini F, Sadough SA, Pouyafar V et al (2013) The rheological behavior of HS6-5-2 tool steel for non-isothermal processing. *Solid State Phenom* 193:317–322
78. Hufschmidt M, Modigell M, Petera J (2004) Two-phase simulations as a development tool for thixoforming processes. *Steel Research Int* 75:513–518
79. Jin SD, Hwan OK (2002) Phase-field modelling of the thermo-mechanical properties of carbon steels. *Acta Mat* 50:2259–2268
80. Jing YL, Sumio S, Jun Y (2005) Microstructural evolution and flow stress of semi-solid type 304 stainless steel. *J Mat Proc Tech* 161:396–406
81. Kalaki A, Ketabchi M (2013) Predicting the rheological behavior of AISI D2 semi-solid steel by plastic instability approach. *American J of Mat Eng and Tech* 1:41–45
82. Koke J, Modigell M (2003) Flow behavior of semi-solid metal alloys. *J. Non-Newton Fluid Mech* 112:141–160
83. Kotrbacek P, Horsky J, Raudensky M et al (2000) Experimental study of steel behaviour in process of mushy state deformation. In: *Proceedings of Metal forming, Krakow*

84. Modigell M, Pape L, Maier HR (2006) Rheology of semi-solid steel alloys at temperatures up to 1500 °C. *Solid State Phenom* 117:606–609
85. Modigell M, Pape L, Hufschmidt M (2004) The rheological behavior of metallic suspensions. *Steel Res Int* 75:506–512
86. Monaghan J, Huppert H, Worster M (2005) Solidification using smoothed particle hydrodynamics. *J Comput Phys* 206:684–705
87. Mordechai S (ed) (2011) Application of Monte Carlo method in science and engineering. InTech, Rijeka
88. Nagira T, Gourlay CM, Sugiyama A et al (2011) Direct observation of deformation in semi-solid carbon steel. *Scr Mater* 64:1129–1132
89. Shimahara H, Baadjou R, Kopp R et al (2006) Investigation of flow behaviour and microstructure on X210CrW12 steel in semi-solid state. *Solid State Phenom* 117:189–192
90. Suzuki HG, Nishimura S (1988) Physical simulation of continuous casting of steels. In: Symposium on physical simulation of welding, hot forming and continuous casting. CANMET, Canada
91. Tseng AA, Horsky J, Raudensky M et al (2001) Deformation behavior of steels in mushy state. *Mat and Des* 22:83–92
92. Yekta FH, Vanini SA (2015) Simulation the flow of semi-solid steel alloy using an enhanced model. *Met Mater Int* 21:913–922
93. Alankar A, Mary A (2010) Constitutive behavior of as-cast aluminum alloys AA3104, AA5182 and AA6111 at below solidus temperatures. *Mat Sci Eng* 527:7812–7820
94. Phillion AB, Thompson S, Cockcroft SL et al (2008) Tensile properties of as-cast aluminum alloys AA3104, AA6111 and CA31218 at above solidus temperatures. *Mat Sci Eng* 497:388–394
95. Phillion K, Maijer AB, Cockcroft SL (2009) Constitutive behavior of as-cast magnesium alloy Mg–Al3–Zn1 in the semi-solid state. *Scr Mat* 60:427–430
96. Ramadan M, Takita M, Nomura H (2006) Effect of semi-solid processing on solidification microstructure and mechanical properties of gray cast iron. *Mat Sci Eng A* 417:166–173
97. Bruni C, Mehtedi M, Gabrielli F (2014) Flow curve modelling of a ZM21 magnesium alloy and finite element simulation in hot deformation. *Key Eng Mater* 622–623:588–595
98. Cai B, Karagadde S, Rowley D et al (2015) Time-resolved synchrotron tomographic quantification of deformation-induced flow in a semi-solid equiaxed dendritic Al–Cu alloy. *Scripta Mater* 103:69–72
99. Cai B, Karagadde S, Yuan L et al (2014) In situ synchrotron tomographic quantification of granular and intragranular deformation during semi-solid compression of an equiaxed dendritic Al–Cu alloy. *Acta Mater* 76:371–380
100. Fuloria D, Lee PD (2009) An X-ray microtomographic and finite element modeling approach for the prediction of semi-solid deformation behaviour in Al–Cu alloys. *Acta Mater* 57:5554–5562
101. Kareh KM, Lee PD, Atwood RC et al (2014) Pore behaviour during semi-solid alloy compression: Insights into defect creation under pressure. *Scripta Mater* 89:73–76
102. Sistaninia M, Terzi S, Phillion AB et al (2013) 3-D granular modeling and in situ X-ray tomographic imaging: a comparative study of hot tearing formation and semi-solid deformation in Al–Cu alloys. *Acta Mater* 61:3831–3841
103. Cook R, Grocock PG, Thomas PM et al (1995) Development of the twin-roll casting process. *J Mat Proc Tech* 55:76–84
104. Fan P, Zhou S, Liang X et al (1997) Thin strip casting of high speed steels. *J Mat Proc Tech* 63:792–796
105. Haga T (2002) Semisolid strip casting using a twin roll caster equipped with a cooling slope. *J Mat Proc Tech* 131:558–561
106. Haga T (2001) Semi-solid roll casting of aluminum alloy strip by melt drag twin roll caster. *J Mat Proc Tech* 111:64–68
107. Haga T, Nishiyama T, Suzuki S (2003) Strip casting of A5182 alloy using a melt drag twin-roll caster. *J Mat Proc Tech* 133:103–107

108. Haga T, Suzuki S (2001) A high speed twin roll caster for aluminum alloy strip. *J Mat Proc Tech* 113:291–295
109. Haga T, Suzuki S (2003) A twin-roll caster to cast clad strip. *J Mat Proc Tech* 138:366–371
110. Haga T, Takahashi K (2004) Casting of composite strip using a twin roll caster. *J Mat Proc Tech* 158:701–705
111. Haga T, Suzuki S (2003) Melt ejection twin roll caster for the strip casting of aluminum alloy. *J Mat Proc Tech* 137:92–95
112. Haga T, Suzuki S (2001) Roll casting of aluminum alloy strip by melt drag twin roll caster. *J Mat Proc Tech* 118:165–168
113. Haga T, Suzuki S (2003) Study on high-speed twin-roll caster for aluminum alloys. *J Mat Proc Tech* 144:895–900
114. Haga T, Takahashi K, Ikawa M et al (2003) A vertical-type twin roll caster for aluminum alloy strips. *J Mat Proc Tech* 140:610–615
115. Haga T, Takahashi K, Ikawa M et al (2004) Twin roll casting of aluminum alloy strips. *J Mat Proc Tech* 154:42–47
116. Kuznetsov AV (1999) Parametric study of macrosegregation in the horizontal strip casting process for different cooling rates and different casting speeds. *Heat Mass Transf* 35:197–203
117. Park CM, Kim WS, Park GJ (2003) Thermal analysis of the roll in the strip casting process. *Mech Res Comm* 30:297–310
118. Park JY, Oh KH (2000) Texture and deformation behavior through thickness direction in strip-cast 4.5wt% Si steel sheet. *ISIJ Int* 40:210–215
119. Seo PK, Park KJ, Kang CG (2004) Semi-solid die casting process with three steps die system. *J Mat Proc Tech* 154:442–449
120. Spinelli JE, Tosetti JP, Santos CA et al (2004) Microstructure and solidification thermal parameters in thin strip continuous casting of a stainless steel. *J Mat Proc Tech* 150:255–262
121. Yun M, Loker S, Hunt JD (2000) Twin roll casting of aluminium alloys. *Mat Sci Eng A* 280:116–123
122. Watari H, Davey K, Rasgado MT et al (2004) Semi-solid manufacturing process of magnesium alloys by twin-roll casting. *J Mat Proc Tech* 156:1662–1667
123. Marongiu EC, Lebeouf F, Caro J et al (2010) Free surface flows simulations in pelton turbines using an hybrid SPH-ALE method. *J Hydraul Res* 48:40–49
124. Project Report (AGH Kraków-IMŻ Gliwice), Number: B0–1124, 2001 (not published)
125. Cleary PW, Monaghan JJ (1999) Conduction modelling using smoothed particle hydrodynamics. *J Comput Phys* 148:227–264
126. Gingold RA, Monaghan JJ (1977) Smoothed particle hydrodynamics-theory and application to non-spherical stars. *Mon Not R Astron Soc* 181:375–389
127. Lucy LB (1997) A numerical approach to the testing of the fission hypothesis. *Astron J* 82:1013–1024
128. Zhang L, Shen H, Rong Y et al (2007) Numerical simulation on solidification and thermal stress of continuous casting billet in mold based on meshless methods. *Mater Sci Eng* 466:71–78
129. Mingming T, David J (2014) An incompressible multi-phase smoothed particle hydrodynamics (SPH) method for modelling thermocapillary flow. *Int J Heat Mass Transf* 73:284–292
130. Xinrong S, Daisuke S, Kazuhiro N (2013) Cartesian mesh with a novel hybrid WENO/meshless method for turbulent flow calculations. *Comput Fluids* 84:69–86
131. Rogers BD, Longshaw SM (2015) Automotive fuel cell sloshing under temporally and spatially varying high acceleration using GPU-based smoothed particle hydrodynamics (SPH). *Adv Eng Softw* 83:31–44
132. Cleary PW, Ha J, Prakash M et al (2006) 3D SPH flow predictions and validation for high pressure die casting of automotive component. *Appl Math Model* 30:1406–1427

133. Cartwright BK, Chhor A, Groenenboom P (2010) Simulation of a helicopter ditching with emergency flotation devices. 5th international Spheric workshop, Manchester, 2010
134. Pineau F, D'Amours G (2011) Application of LS-DYNA SPH formulation to model semi-solid metal casting. 8th European LS-DYNA Users Conference, Strasbourg
135. Pineau F, D'Amours G (2012) SPH model approach used to predict skin inclusions into semisolid metal castings. Modeling and simulation in materials processing. Wiley, Hoboken
136. Cleary PW, Prakash M, Das R et al (2012) Modelling of metal forging using SPH. Appl Math Model 36:3836–3855
137. Jianga F, Oliveiraa M, Sousaa ACM (2007) Mesoscale SPH modeling of fluid flow in isotropic porous media. Comput Phys Commun 176:471–480
138. Limido J, Espinosa C, Salaun M et al (2011) Metal cutting modelling SPH approach. Int J Mach Mach Mater 9:177–196
139. Xu J, Wang J (2014) Interaction methods for the SPH parts in LS-DYNA. 13th International LS-DYNA Users Conference, Detroit
140. Rabczuk T, Xiao SP, Sauer M (2006) Coupling of mesh-free methods with finite elements: basic concepts and test results. Com Num Met Eng 22:1031–1065
141. Mitsume N, Yoshimura S, Murotani K et al (2015) A hybrid finite element and mesh-free particle method for disaster-resilient design of structures. International workshop on Nuclear safety, Berkeley, 22–24 March 2015
142. Lewis RW, Roberts PM (1987) Finite element simulation of solidification problems. Appl Sci Res 44:61–92
143. Voller VR, Swaminathan CR, Thomas BG (1990) Fixed grid techniques for phase change problems: a review. Intern J Numer Methods Eng 30:875–898
144. Gandin ChA, Rappaz M (1994) A coupled finite element-cellular automaton model for the prediction of dendritic grain structures in solidification processes. Acta Metall 42:2233–2246
145. Gandin ChA, Rappaz M (1997) A 3D cellular automaton algorithm for the prediction of dendritic grain growth. Acta Metall 45:2187–2195
146. Gandin CHA, Desbiolles JL, Rappaz M et al (1999) A three-dimensional cellular automaton-finite element model for the prediction of solidification grain structures. Metall Mater Trans 30A:3153–3165
147. Rappaz M, Gandin CHA, Desbiolles JL et al (1996) Prediction of grain structures in various solidification processes. Metall Mater Trans 27A:695–705
148. Brown SGR, Brucet NB (1995) Three-dimensional cellular automaton models of microstructural evolution during solidification. J Mater Sci 30:1144–1150
149. Chan V (ed) (2013) Theory and application of Monte Carlo simulation. InTech, Rijeka
150. Das A, Fan Z (2004) A Monte Carlo simulation of solidification structure formation under melt shearing. Mater Sci Eng 36:330–335
151. Mode JC (ed) (2011) Application of Monte Carlo methods in biology, medicine and other field of science. InTech, Rijeka
152. Carron D et al (2010) Modelling of precipitation during friction stir welding of an Al–Mg–Si alloy. Tech Mech 30:29–44
153. Li MY, Kannatey EA (2002) Monte Carlo simulation of heat-affected zone microstructure in laser-beam-welded nickel sheet. Weld J 81:1–12
154. Raabe D (2000) Scaling Monte Carlo kinetics of the potts model using rate theory. Acta Mater 48:1617–1628
155. Loren S, Svensson T (2012) Second moment reliability evaluation vs. Monte Carlo simulations for weld fatigue strength. Qual Reliab Eng Intern 28:793–991
156. Amitabha D, Eric JM (2001) A Monte Carlo simulation of solidification structures of binary alloys. Philos Mag A 11:2725–2742
157. Das A, Ji S, Fan Z (2002) Morphological development of solidification structures under forced fluid flow: a Monte-Carlo simulation. Acta Mater 18:4571–4585
158. Gao J, Thompson RG (1996) Monte Carlo simulation of solidification. Acta Met 44:77–86

159. Gao J, Thompson RG (1996) Real time-temperature models for Monte Carlo simulations of normal grain growth. *Acta Met* 44:4565–4570
160. Maazi N (2017) Conversion of Monte Carlo steps to real time for grain growth simulation. *Adv Math Phys* 2017:1–8
161. Mishra S, DebRoy T (2004) Measurements and Monte Carlo simulation of grain growth in the heat-affected zone of Ti–6Al–4 V welds. *Acta Mater* 52:1183–1192



<http://www.springer.com/978-3-319-67975-4>

Modeling Steel Deformation in the Semi-Solid State

Hojny, M.

2018, XV, 302 p. 237 illus., 167 illus. in color.,

Hardcover

ISBN: 978-3-319-67975-4